MOTION ARTIFACT REMOVAL IN ECG SIGNALS USING MULTI-RESOLUTION THRESHOLDING

Falco Strasser[1], Michael Muma[2] and Abdelhak M. Zoubir[1,2]

[1] Graduate School CE,
Technische Universität Darmstadt
Dolivostr. 15, D-64293 Darmstadt Germany
Email: strasser@gsc.tu-darmstadt.de

[2] Signal Processing Group,
Technische Universität Darmstadt
Merckstr. 25, D-64283 Darmstadt Germany
Email: {muma,zoubir}@spg.tu-darmstadt.de

ABSTRACT

The electrocardiogram (ECG) is a powerful non-invasive tool which allows for diagnosis of a wide range of heart conditions. Today, portable ECG recording devices, equipped with a transmitter, can be used to provide health related information and to trigger alarms in case of life threatening situations. However, these devices suffer from motion induced artifacts. While much research has been conducted to remove time invariant noise, the removal of motion induced artifacts remains an unsolved problem. We therefore introduce a new method which removes these artifacts. This is done by obtaining an estimate of the artifacts using the stationary wavelet transformation. An automatic multi-resolution thresholding scheme which uses a robustified QRS detection is proposed. Real data examples as well as simulations are given which illustrate the performance of the method.

Index Terms— ECG, motion induced artifacts, outliers, stationary wavelet transform

1. INTRODUCTION

The electrocardiogram (ECG) is a non-invasive diagnostic tool to record the electrical activity of the heart. This is done by measuring the potential difference between several electrodes which are placed on the skin at predefined points of the human body. One cycle of the ECG represents the depolarization/repolarization of the atrium and the ventricle which occurs for every heartbeat. These appears as P wave, QRS complex and T wave, see Figure 1. ECG is used to detect abnormalities, such as heart arrhythmia. For automated signal processing methods, as well as for clinicians, it is important that the ECG recordings are noise free and not corrupted by outliers, if possible [1]. However, it is not always possible to produce clean measurements. For an ECG recording, a simple movement by the patient creates a significant artifact [2]. This is illustrated in Figure 1, where the left arm has been moved. The example was recorded at our lab using a one lead configuration with $f_s = 100$Hz. The figure depicts a typical motion induced artifact which occurs approximately
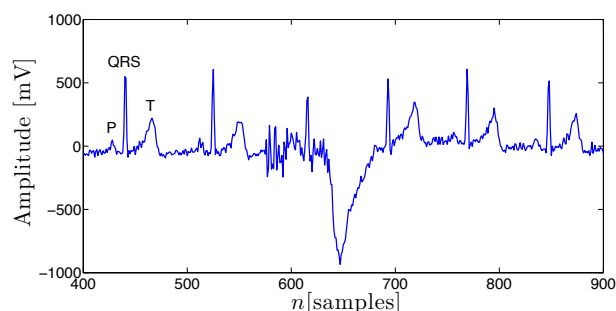

Fig. 1. ECG signal with patient motion induced artifacts and impulsive noise due to arm movement approximately between 570 and 680 samples.

from $630 < n < 680$ and is preceded by impulsive noise. Today, portable ECG recording devices, equipped with a transmitter, can be used to provide health related information and to trigger alarms in case of life threatening situations. Most existing work in ECG de-noising effectively removes contaminants such as power line interference, contact noise or baseline wandering, see e.g. [3] for an overview of recent research. In [3], Li and Lin introduced an optimal de-noising algorithm for ECG signals which uses the stationary wavelet transform (SWT). This is achieved by finding the best combination and parameters of previously proposed SWT-based methods of ECG signal de-noising. In Figure 2 the result of this algorithm for the previously mentioned ECG recording is depicted. The invariant noise of the recording is removed. However, the example shows that the algorithm is not robust against motion induced artifacts and impulsive noise. This therefore constitutes the focus of our work. Pawar et al. proposed a method to classify and reduce these artifacts [4]. However, their method requires patient specific training data for the different types of movements, which is a drawback. Obtaining the training data for each patient is very time consuming. Furthermore, due to the non-stationarity of ECG signals [5] and artifacts, the characteristics may change over time. Hence, we propose a robust method to remove motion induced artifacts which works fully automatically and
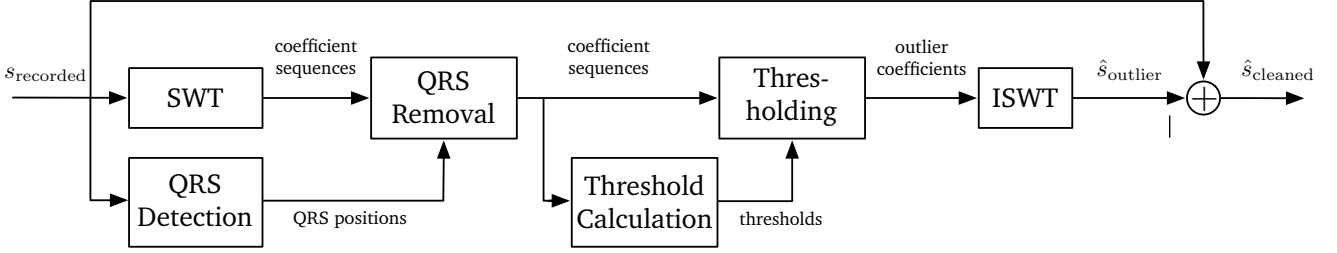
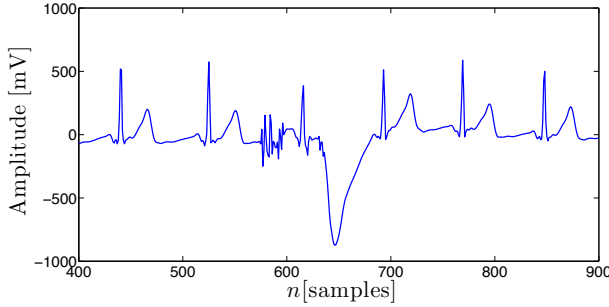**Fig. 3**. Scheme of the multi-resolution thresholding algorithm.

Fig. 2. Result of ECG recording (Figure 1) using the optimal de-noising algorithm proposed in [3], which is clearly not robust against motion induced artifacts.

independent of the specific patient and recording. To achieve this, we use the stationary wavelet transform which allows for a better separation of signal and artifacts than time or frequency based methods.

Our paper is organized as follows. We start with a description of the algorithm in Section 2. Then we show some results in Section 3 followed by the conclusion and future work in Section 4.

2. ALGORITHM

The idea of our algorithm is to estimate a signal $\hat{s}_{\text{outliers}}(n)$, which represents the motion induced artifacts and impulsive noise. This signal is then subtracted from the recorded signal to get a cleaned ECG signal:
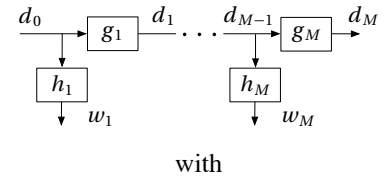
$$\hat{s}_{\text{cleaned}}(n) = s_{\text{recorded}}(n) - \hat{s}_{\text{outliers}}(n), n = 1, \ldots, N. \quad (1)$$

This is well motivated, since motion induced artifacts are additive disturbances. We use the diversity of the coefficient sequences obtained by the SWT and a multi-resolution thresholding methodology to estimate $\hat{s}_{\text{outliers}}(n)$. The scheme of the algorithm is shown in Figure 3. The single blocks are described in the following.

2.1. Stationary Wavelet Transform (SWT)

The algorithm starts with the SWT. It is a powerful tool for non-stationary signals [6], such as ECG signals. In our ap-

proach, we use the SWT for two reasons: (i) The SWT is invariant against shifts of the signal in the time domain. The digital wavelet transform (DWT), which is also used for ECG signal de-noising [7], can not provide this feature. This becomes critical for detecting specified signal components like motion induced artifacts and outliers as well as QRS complexes. (ii) The decimation of the coefficients at each level of the transformation algorithm is omitted, more samples in the coefficient sequences are available and hence a better outlier detection can be performed. The implementation of the SWT, which is based on the pyramid algorithm introduced by Mallat [8], is depicted in Figure 4. The wavelet coefficients are given by the sequences $\{w_1, w_2, \ldots, w_M\}$ and the scaling coefficients by the sequences $\{d_1, d_2, \ldots, d_M\}$, where M denotes the order of the SWT. h_s and g_s are the impulse responses of the high- and low-pass filters, which are upsampled by a factor of two at each stage $s = 1, 2, \ldots, M$. To represent the signal we need all wavelet coefficient sequences and the scaling coefficients at level M. Extensive empirical

with

Fig. 4. Overview of the implementation of the SWT [8] which is shift invariant.

evaluations have shown that the choice of the mother wavelet has little impact on the performance of our algorithm. Hence, we use the simplest mother wavelet, the Haar wavelet. Also we set $M = 5$ as in [3], which provides a good trade off between the amount of available information and computational effort. Figure 5 shows the SWT of the exemplary recorded ECG signal, see Figure 1, using the above described parameters. Additionally to the ECG signal, the wavelet coefficients and the scaling coefficients are displayed. The first three coefficient sequences mostly represent the fast changing parts of the signal, like the QRS complexes and the oscillating noise. The last three sequences contain information of slow changes
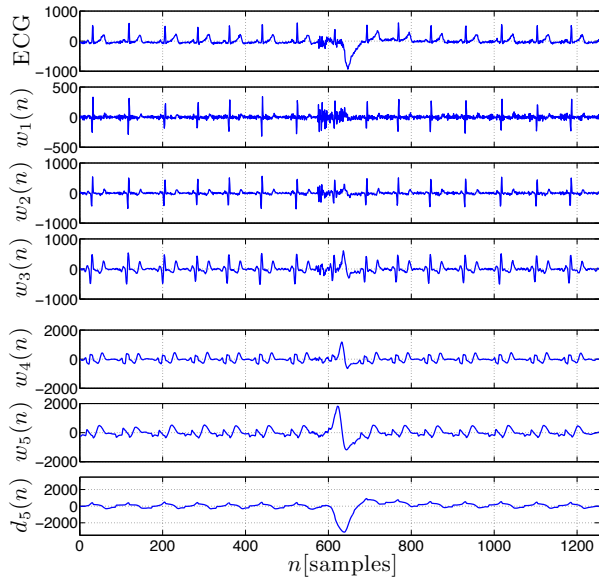
Fig. 5. SWT of the ECG signal from Figure 1. The diversity of the coefficient sequences can be used to separate signal and outliers.

in the signal, due to the P and T waves and the motion induced artifact. To obtain the coefficients, which represent the outliers, we compute upper and lower thresholds using robust statistics [9] for each coefficient sequence. For $w_4(n)$, $w_5(n)$ and $d_5(n)$ this is straight forward. For $w_1(n)$, $w_2(n)$ and $w_3(n)$ the outliers are masked by the coefficients representing the QRS complexes. In order to overcome this problem, we detect the QRS complexes and remove them from the first three coefficient sequences before calculating the thresholds. The QRS detection and removal is described in the next section.

2.2. QRS detection

The QRS detection is based on the method proposed in [10] with some modifications: At first, the wavelet shrinkage method developed by Donoho and Johnstone [11] is used to denoise the signal. The denoised signal is then filtered by a high-pass in order to suppress the P and T waves. After this, the QRS feature signal $z(n)$, which represents the energy over a window, is computed. To detect the QRS complexes a threshold T_{QRS} is used. Since the threshold proposed by Chen et al. is not robust against motion induced artifacts, we define a new threshold. First, we split $z(n)$ into equally long segments and calculate the maximum of each segment. Then we compute the threshold by $T_{QRS} = \hat{\mu}(\mathrm{maxima}) - c \cdot \hat{\sigma}(\mathrm{maxima})$. Robust estimates of the mean μ and scale σ, i.e. the median and the normalized median absolute deviation (MADN) are used [12, 9]. The constant c should be chosen greater or equal to 2 which ensures to detect all QRS complexes. The choice of c depends
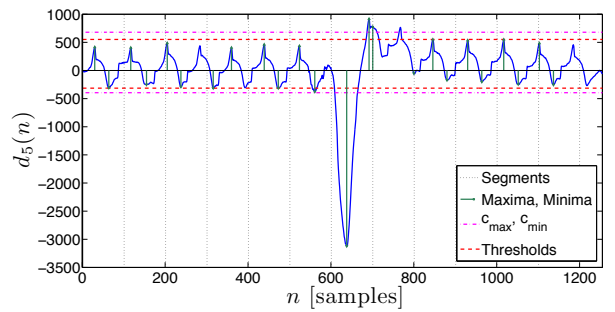

Fig. 6. Threshold calculation illustrated for $d_5(n)$.

on the prior knowledge of the amount of impulsive noise in the data. If it is likely that there is almost no impulsive noise in the data, c can be chosen greater than 2.5. In case of impulsive noise $2 \le c \le 2.5$ is recommended. The choice of segment length should provide that each segment contains roughly one QRS complex. Since the typical resting heart rate for adults is 60-90 beats per minute, we choose a segment length of 1 second. If $z(n) \ge T_{QRS}$, a QRS complex is detected. Hence, we get the QRS positions and set all coefficients in $w_1(n)$, $w_2(n)$ and $w_3(n)$ at these positions to zero. In a small number of cases, two or zero QRS complexes may occur in one segment. However, the robust location and scale estimates in the calculation of T_{QRS} can easily deal with this. Now we are able to separate the outliers from the clean signal by thresholding. The threshold calculation is explained in the following section.

2.3. Threshold Calculation

We calculate an upper and a lower threshold for all coefficient sequences to separate the outliers from the original ECG signal. For this, we split each sequence into segments analogous to Section 2.2. Then we calculate the maximum and minimum of each segment. With this procedure we obtain several maxima and minima of each sequence. From this set, we define $c_{\max} = \hat{\mu}(\mathrm{maxima}) + \hat{\sigma}(\mathrm{maxima})$ and $c_{\min} = \hat{\mu}(\mathrm{minima}) - \hat{\sigma}(\mathrm{minima})$. Again, robust estimates for the mean μ and the scale σ are used. Then, the upper threshold T_u is given by the largest maxima, which is below $c_{\max}$. Accordingly, the lower threshold T_l is the smallest minima above $c_{\min}$. To illustrate the threshold calculation, Figure 6 depicts the example of the coefficient sequence $d_5(n)$ and displays the edges of the segments, $c_{\max}, c_{\min}, T_u$ and T_l.

2.4. Thresholding and Inverse SWT (ISWT)

After calculating the thresholds for each stage, we perform hard thresholding to obtain a representation of the outlier signal in the wavelet domain, which is given by the following
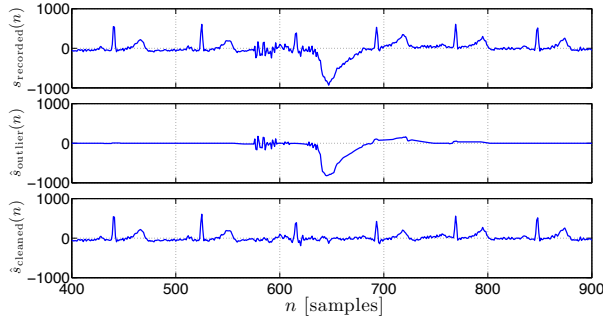
Fig. 7. The multi-resolution thresholding algorithm gives $\hat{s}_{\text{outlier}}(n)$ (middle), which is substracted from the $s_{\text{recorded}}(n)$ (top) to obtain the cleaned signal $\hat{s}_{\text{cleaned}}(n)$ (bottom).

equations:

$$\hat{w}_s^*(n) = \begin{cases} w_s(n), & \text{if } d_s(n) > T_{s,u} \\ w_s(n), & \text{if } d_s(n) < T_{s,l} \\ 0, & \text{otherwise.} \end{cases}$$

and

$$\hat{d}_M^*(n) = \begin{cases} d_M(n), & \text{if } d_M(n) > T_{d,u} \\ d_M(n), & \text{if } d_M(n) < T_{d,l} \\ 0, & \text{otherwise} \end{cases}$$

Computing ISWT using the coefficient sequences of the outliers yields $\hat{s}_{\text{outliers}}(n)$. The cleaned ECG signal $\hat{s}_{\text{cleaned}}(n)$ is computed by using Eq. (1). The result is shown in Figure 7, where the recorded ECG, the estimated outlier signal and the cleaned ECG are displayed. The motion induced artifact and the impulsive noise are almost completely canceled out.

3. RESULTS

All datasets and algorithms are available at www.spg.tu-darmstadt.de/res/dl/. As discussed in the previous sections, we use the following parameters: Haar wavelet and $M = 5$ stages for the SWT, segment length $= 1$ second and $c = 2$ to calculate T_{QRS}. To illustrate the performance of the method, we compared our method with the algorithm proposed by Li and Lin [3]. For this, we used a method proposed by McSharry et al. in [13] to generate synthetic ECG signals. The model generates an ECG with a time-varying amplitude of the R peak equal approximately to 1 and allows to vary the ECG characteristics such as heart rate and LF/HF ratio. Synthetic motion artifacts are modeled by an additive patchy outlier model using a moving average (MA) process driven by impulsive noise which is defined by $v(n) = b_0\tilde{v}(n) + b_1\tilde{v}(n-1) + \ldots + b_q\tilde{v}(n-q)$, where q is the order of the MA process. The sequence $\tilde{v}(n)$ is given by $\tilde{v}(n) \sim (1-\varepsilon)\delta_0 + \varepsilon\mathcal{N}(0, \sigma_v^2)$, δ_0 is a point mass distribution located at zero and $\mathcal{N}(0, \sigma_v^2)$ is a zero mean Gaussian

with variance σ_v^2. The parameter ε denotes the probability of an outlier to occur and σ_v^2 represents the impulsiveness of the outliers. We set $\varepsilon = 0.05$ and $\sigma_v = 1$. $\{b_0, b_1, \ldots, b_q\}$ determines the temporal structure (shape) of the outliers. For the simulation we choose a parabola, which resembles typical motion induced artifacts. The length of the outlier blocks varies randomly from $0.1s$ to $1.5s$. We performed a Monte Carlo simulation, where we generated 1000 different synthetic ECG signals, which were then disturbed with motion artifacts. To compare the results of our method and Li and Lin [3], we calculated the mean square error (MSE) between the signals corrupted with outliers and the original ECGs. We did the same with the cleaned signals using both algorithms. In the following table the average MSEs are given:

	Uncleaned	Li and Lin	Multi-res. thres.
av. MSE	0.0134	0.0141	0.0025

The results confirm the statement in Section 1, that the optimal de-noising algorithm by Li and Lin is not able to reduce motion induced artifacts. Our proposed algorithm reduces the average MSE by a factor of 5.36. The increase of the average MSE by using Li and Lin can be explained, by the fact that the method reduces the peaks of the signals. Additionally, we considered real ECG data to evaluate our algorithm. For this, we selected 19 recordings of 1 minute duration which do not contain outliers from the MIT-BIH Arrhythmia Database. We corrupted them with the synthetic patchy outliers with the same parameters as in the previous case except for $\sigma = 350$, which had to be adjusted to the amplitudes of the database. For all recordings, we performed a Monte Carlo simulation with 100 iterations. The average MSE for the corrupted signals is 3033.4 and for the cleaned signals it is 467.6, which results in a reduction factor of 6.49. In a further study, we used real motion artifacts obtained from the MIT-BIH Noise Stress Test Database. From this database we chose 6 artifacts and corrupted each of the 19 recordings with each of the 6 artifacts. Then again the MSEs were calculated. This results in an average MSE of 1384.2 for the corrupted signals and 479.48 for the cleaned signals. Hence, the average MSE is reduced by a factor of 2.89. These studies show that our algorithm deals very well not only with normal ECGs but also with ECGs containing heart arrhythmias. In addition to the MSE studies, we evaluated our algorithm by visual examination of real ECG signals, which we recorded at our lab. Here, two examples are shown. Figure 7 depicts the result of the proposed algorithm for the signal displayed in Figure 1. It is clear to see that the oscillating noise is suppressed and the movement artifact is canceled out. Also the non-corrupted parts are nearly untouched. However, the T wave at $n \approx 625$ could not be reconstructed. Figure 8 illustrates how the proposed method handles a slow movement, which results in a large patch of outliers. The method handles this situation very well. All QRS complexes are recovered, the T waves are visible and the baseline is corrected as well. To assess the gain of our method as a preprocessing step for R peak detection,
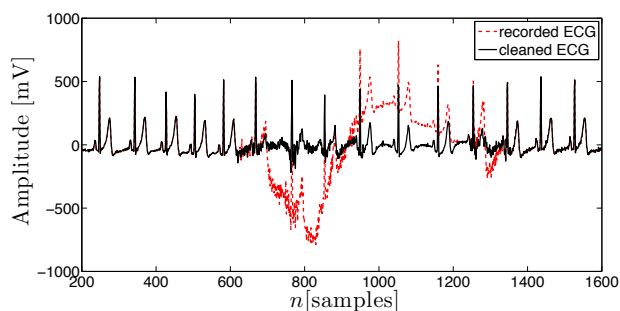
Fig. 8. ECG with artifact from slow movement of the arm (red) and cleaned ECG signal (black).

we used the method proposed in [14] on the data given by the 19 recordings and synthetic motion artifacts. The average detection and false alarm rates are shown in the following table:

	Av. detection rate	Av. false alarm rate
Corrupted ECGs	99.49%	4.03%
Clean ECGs	99.53%	0.1%

We see the detection rate is not much influenced by the outliers, hence there is no difference between the ECGs with outliers and the cleaned ECGs. However, due to the outliers some false alarms occur which are omitted by using our method. This shows that our algorithm is useful as preprocessing tool to enhance ECG analysis.

4. CONCLUSION

A new method to detect and to remove outliers in ECG data generated by movement of the patient has been introduced. It is able to recover corrupted QRS complexes and removes temporary baseline shifts. In addition, it suppresses impulsive noise. We also showed that our algorithm can improve R peak detection methods which emphasizes its applicability as a preprocessing tool in automated ECG analysis. The suggested method is an effective, robust, consistent and computationally cheap algorithm which does not require training data and works fully automatic and independent of the specific subject. Additionally, the adaption to a real-time system is possible. Hence, in the future, this method could be used in portable recording devices. Future and ongoing work include a multi-resolution modeling algorithm, which uses a different mother wavelet to generate wavelet coefficient sequences, which have a structure that is suitable for model-based outlier detection and signal reconstruction.

5. REFERENCES

[1] R. Rangayyan, *Biomedical Signal Analysis (A Case-Study Approach)*, Wiley-IEEE Press, 2002.

[2] A.M. Zoubir, V. Koivunen, Y. Chakhchoukh and M. Muma, "Robust estimation in signal processing," *IEEE Signal Process. Mag.*, 2012.

[3] S. Li and J. Lin, "The optimal de-noising algorithm for ECG using stationary wavelet transform," *WRI World Cong. on Computer Science and Inform. Eng.*, vol. 6, pp. 469 –473, 2009.

[4] T. Pawar,, S. Chaudhuri, and S.P. Duttagupta, "Body movement activity recognition for ambulatory cardiac monitoring," *IEEE Trans. Biomed. Eng.*, vol. 54, no. 5, pp. 874 –882, 2007.

[5] M. Muma, D.R. Iskander and M.J. Collins, "The role of cardiopulmonary signals in the dynamics of the eye's wavefront aberrations," *IEEE Trans. Biomed. Eng.*, vol. 57, no. 2, pp. 373 –383, 2010.

[6] S.G. Mallat, *A Wavelet Tour of Signal Processing*, Elsevier, 2006.

[7] B.N. Singh and A.K. Tiwari, "Optimal selection of wavelet basis function applied to ECG signal denoising," *Digital Signal Processing*, vol. 16, no. 3, pp. 275 – 287, 2006.

[8] S.G. Mallat, "A theory for multiresolution signal decomposition: the wavelet representation," *IEEE Trans. Pattern Anal. Mach. Intell.*, vol. 11, no. 7, pp. 674 –693, 1989.

[9] P.J. Huber and E.M. Ronchetti, *Robust Statistics*, John Wiley & Sons, Inc., 2009.

[10] S.-W. Chen, H.-C. Chen and H.-L. Chan, "A real-time QRS detection method based on moving-averaging incorporation with wavelet denoising," *Comput. Meth. Prog. Biomed.*, vol. 82, no. 3, pp. 187 – 195, 2006.

[11] D.L. Donoho and I.M. Johnstone, "Ideal spatial adaptation via wavelet shrinkage," *Biometrika*, vol. 81, no. 3, pp. 425–455, 1994.

[12] M. Muma and A.M. Zoubir, "Robust model order selection for corneal height data based on τ estimation," in *IEEE International Conference on Acoustics, Speech and Signal Processing (ICASSP)*, 2011, pp. 4096 –4099.

[13] P.E. McSharry, G.D. Clifford, L. Tarassenko and L.A. Smith, "A dynamical model for generating synthetic electrocardiogram signals," *IEEE Trans. Biomed. Eng.*, vol. 50, no. 3, pp. 289 –294, 2003.

[14] P.S. Hamilton and W.J. Tompkins, "Quantitative investigation of QRS detection rules using the MIT/BIH arrhythmia database," *IEEE Trans. Biomed. Eng.*, vol. 33, no. 12, pp. 1157 –1165, 1986.